coatings

MDPI

Article

Micron-Smooth, Robust Hydrophobic Coating for Photovoltaic Panel Surfaces in Arid and Dusty Areas

Rongrong Guo [1,2], Yuanhao Wang [1,3,*], Hao Lu [1,2,4,*], Shifeng Wang [5,*], Bohan Wang [6] and Qiyu Zhang [7]

[1] Center of New Energy Research, School of Future Technology, Xinjiang University, Urumqi 830047, China; guorongrongmail@163.com
[2] Engineering Research Center Northwest Energy Carbon Neutrality, Ministry of Education, Xinjiang University, Urumqi 830047, China
[3] Hoffmann Institute of Advanced Materials, Shenzhen Polytechnic University, Shenzhen 518055, China
[4] School of Electrical Engineering, Xinjiang University, Urumqi 830047, China
[5] Innovation Laboratory of Materials for Energy and Environment Technologies, Institute of Oxygen Supply, College of Science, Tibet University, Lhasa 850000, China
[6] College of Science (Managerial Economic Programme), Nanyang Technological University, South Spine, Singapore 639798, Singapore
[7] Department of Economics, Huron University College, London, ON N6G 1H3, Canada
* Correspondence: wangyuanhao@szpu.edu.cn (Y.W.); luhao@xju.edu.cn (H.L.); wsf@utibet.edu.cn (S.W.)

Abstract: Photovoltaic (PV) power generation is a clean energy source, and the accumulation of ash on the surface of PV panels can lead to power loss. For polycrystalline PV panels, self-cleaning film is an economical and excellent solution. However, the main reasons why self-cleaning coatings are currently difficult to use on a large scale are poor durability and low transparency. It is a challenge to improve the durability and transparency of self-cleaning thin films for PV panel surface against ash accumulation. Therefore, in this paper, a resin composite film containing modified silica components was designed and synthesized, mainly by the organic/inorganic composite method. A transparent hydrophobic coating with nano-micro planar structures was constructed, which primarily relies on the hydrophobic properties of the compound itself to build the hydrophobic oleophobic coating. The layer has a micrometer-scale smooth surface structure and high transparency, with a 0.69% increase in light transmittance compared with uncoated glass, and the durability is good. It is mainly applied to the surface of photovoltaic devices, which can alleviate the dust accumulation problem of photovoltaic panels in arid, high-temperature, and dusty areas and reduce the maintenance cost of them.

Keywords: self-cleaning; hydrophobic; transparency; photovoltaic; robust; friction resistant

Citation: Guo, R.; Wang, Y.; Lu, H.; Wang, S.; Wang, B.; Zhang, Q. Micron-Smooth, Robust Hydrophobic Coating for Photovoltaic Panel Surfaces in Arid and Dusty Areas. *Coatings* **2024**, *14*, 239. https://doi.org/10.3390/coatings14020239

Academic Editor: Joachim Albrecht

Received: 23 January 2024
Revised: 10 February 2024
Accepted: 17 February 2024
Published: 18 February 2024

1. Introduction

With the deterioration in global climate and environmental problems in recent years, replacing traditional fossil energy with clean energy has become a research focus and difficulty. The photovoltaic industry has become a pillar of the new energy industry with its advantages of safety, green, and renewable [1]. However, studies have shown that in dusty or polluted climates, which can produce dust accumulation on PV panels [2], the actual power output may be reduced by as much as 60% if the PV panels are not cleaned regularly [3]. Therefore, the problem of dust accumulation on PV panels is particularly prominent in dry, high-temperature, and dusty areas [4]. Ash accumulation not only leads to a decrease in power generation efficiency but also to localized overheating of the solar panel surface, which then causes hot spots, leading to module damage and affecting the life of the PV installation [5].

Currently, the most common methods reduce the loss from dust accumulation are to change the tilt of the photovoltaic panels (to find the best angle) and/or regular cleaning of the photovoltaic panels [6], the disadvantage is that these will increase water consumption

and increase the maintenance costs in terms of labor. So, various self-cleaning films have been proposed for reducing dust accumulation on the surface of solar panels because nano-self-cleaning films are a more economical and convenient way to minimize dust accumulation [7].

The self-cleaning performances and mechanisms of superhydrophobic and superhydrophilic coatings on solar photovoltaic cells have been compared by experimental measurement [8]. It was demonstrated that hydrophobic, superhydrophobic, hydrophilic, and superhydrophilic coatings have good self-cleaning ability [8]. Self-cleaning films for solar panel surfaces are mainly categorized into hydrophobic and hydrophilic films. The self-cleaning principle of hydrophobic self-cleaning film is as follows: (1) hydrophobicity means dust and pollutants do not easily attach to the surface. (2) Through the natural action of wind and rain, dust can be better removed from the surface of solar panels. The principle of hydrophilic self-cleaning film is that water is wholly diffused on the surface, and with the flow of water, dust can be quickly taken away [9].

Hydrophobic films are more suitable in dry and dusty water-scarce areas because dust sources are mainly microscopic particles of soil and rocks, bird droppings, fungal algae, pollen, and artificial sources, specifically, industrial and traffic dust [10]. Hydrophobic films have the more obvious advantage of reducing aqueous and pollutant deposition. Currently, hydrophobic films have promising applications in the steel, textile, and petroleum industries, anti-fingerprint screens, microfluidic devices, and oil/water separation membranes. Many methods and properties for the preparation of superhydrophobic coatings have been reported in the literature. The basic principles of superhydrophobicity are (1) the construction of rough structures on the surface, and (2) the chemical modification of low-surface-energy compounds. So, the most common approach is to combine micron- or nanoscale rough structures with low-surface-energy coatings. Rough structures can be constructed by constructing functionalized silica nanoparticles [11,12]; or using other etching methods to construct pyramidal, conical, and prismatic micro- and nanoscale rough structures [13]. Low-surface-energy surfaces can be achieved using silyl surface modification, as proposed by Barry Arkles, which is widely used [14]; fluorine-chemistry-based surface modification materials are also widely used for their excellent hydrophobic properties [15]. Fluorine compounds with low surface energy combined with alkylsilanes result in more hydrophobic materials, with contact angles as high as 169° [16]. The preparation of many coatings also focuses on modified silica because silica-based materials are ideal for forming superhydrophobic coatings as they offer a tunable refractive index and thickness with excellent adhesion to the base substrate [17].

It can be found that the hydrophobic properties of materials reported in many studies were achieved by surface modification [18], and by forming covalent bonds to improve weather resistance [19]. So self-cleaning film is currently challenging to apply on large areas mainly because of poor durability and low transparency; with the surface mechanical structure in daily cleaning and maintenance as well as the wear and tear caused by wind, rain, sand, and gravel under natural conditions, the hydrophobic performance of the coating decreases substantially. And the high cost of most coatings, coating methods, and the complexity of the coating process are the most significant constraints on the practical application of self-cleaning coatings. The future development in the field of self-cleaning coatings is to focus on the development of reliable methods that are easy-to-handle, cost-effective, stable, and durable for self-cleaning coating applications [20].

Therefore, this paper mainly constructs a transparent hydrophobic coating with micro- and nano-level smooth surface structures. A smooth surface prevents scratches. The principle is to make objects slide across the surface instead of scratching the paint film. So smooth surfaces demonstrate significant scratch resistance. The solution mainly relies on the hydrophobic property of the compound itself to construct the hydrophobic and oleophobic coating, which has a micron-level flat surface. A hydrophobic coating was constructed by an organic/inorganic composite method using hydrophobic precursor particles polymerized with organic resins in a strict proportion. The preparation and coating methods are simple,

easy to use, and have low manufacturing costs. The hydrophobic coating was verified to have strong resistance to physical friction, a transparency enhancement effect, and both good durability and transparency. So, the wear and tear in daily cleaning and maintenance have less impact on the hydrophobicity of the surface, thus achieving the requirements of high durability and low maintenance costs. It provides a solution to the problem of ash accumulation on photovoltaic panels in arid, high-temperature, and dusty areas.

2. Materials and Methods

2.1. Materials

The primary materials used in the experiment are listed in Table 1.

Table 1. Main materials used in the experiment.

Material Name	Reagent Purity (wt.%)	Manufacturer
SiO_2 (15–20 nm)	>99.9%	Shanghai Aladdin Biochemical Technology Co., Ltd. (Shanghai, China)
Hexadecyltrimethoxysilane (HDTMS)	>85%	Shanghai Maclean Biochemical Technology Co. (Shanghai, China)
Tetraethyl orthosilicate (TEOS)	98%	Shanghai Maclean Biochemical Technology Co. (Shanghai, China)
Triethoxymethylsilane (METEOS)	98%	Shanghai Maclean Biochemical Technology Co. (Shanghai, China)
Sylgard184 elastomer base and curing agent	2%	Dow corning (Shanghai, China)
106 silicone resin	/	Zongyang Sanjin Pigment Co., Ltd. (Zongyang, China)
Dichloromethane	Analytical reagent	Tianjin Jindong Tianzheng Chemical Reagent Factory. (Tianjin, China)
n-Heptane	>99%	Tianjin Fuchen Chemical Reagent Factory. (Tianjin, China)
Ethanol	>99.7%	Tianjin Fuchen Chemical Reagent Factory. (Tianjin, China)
H_2O	/	Tianjin Fuchen Chemical Reagent Factory. (Tianjin, China)
HCl	36%–38%	Tianjin Fuchen Chemical Reagent Factory. (Tianjin, China)

2.2. Preparation

2.2.1. Preparation of Hydrophobic Precursor Particles

Firstly, 50 mL of HCl (0.01 mol/L) was added into a clean beaker and stirred on the magnetic agitator. At the same time, 0.06 g of SiO_2 was put into the beaker slowly, then stirred at 600 r/min for 10 min. Secondly, 2.8 g of METEOS, 8.7 g of HDTMS, and 5.2 g of TEOS were added into the mixture, then stirred at 500 r/min for 18 h under room temperature; a white suspension was obtained. Finally, the white powder was washed three times with deionized water, and then, the white powder was put into the electric constant-temperature blast-drying oven at 60 °C to dry for 24 h (Figure 1).

2.2.2. Preparation of Transparent Film

Firstly, slides were pretreated before coating them with the film. They were ultrasonically cleaned in ethanol and distilled water 3 times.

Secondly, 0.1 g of the white particles made in the first step was added into a three-necked flash, 106 silicone resin, sylgard184, curing agent, 5 mL of dichloromethane, and 6 mL of n-heptane were put into a 50 mL three-necked flask in the given order, and stirred at room temperature for 30 min (Figure 1).

Finally, 0.2 mL of the mixture was taken with a pipette and applied onto a 25.4 mm × 76.2 mm clear glass sheet. The glass was put into the drying oven at 150 °C for curing for 4 h.

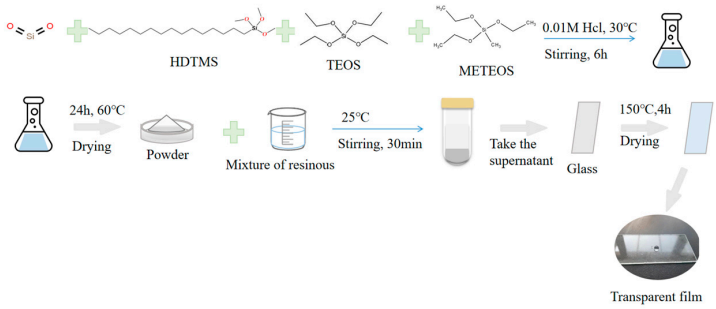

Figure 1. The preparation procedure for transparent film.

3. Results

3.1. Microscopic Morphology and Chemical Composition Test

Scanning electron microscopy (SEM, JSM-7500F, Tokyo, Japan) was used to examine the microscopic morphology of the prepared coatings. Fourier transform infrared (FT-IR) spectra were measured with a Fourier transform infrared spectrometer (NEXUS, Thermonics Co., Madison, WI, USA). EDX (JSM-7800F prime, Tokyo, Japan) spectroscopy was used to determine the elemental content of the specimens. Transmission electron microscopy (TEM, FEI Tecnai G2 F30, Hillsboro, OR, USA) was used to determine the coatings' structures, sizes, and distribution patterns.

Scanning electron microscopy is an essential technical tool to observe the size, shape, and distribution of microstructures on the surface of coatings. As shown in Figure 2a, at a scale of 10 microns, the coating has a small amount of bubbles on the surface, caused by the lack of delicate handling during coating. We recommend that coating is performed by a rotary coating method and the coating process needs to be kept clean. Drying should be performed in a drying oven, keeping the process clean and pressurized if possible. Figure 2b shows a small number of rectangular crystals of 100 nm–200 nm, which is due to the precipitation of crystals produced by inhomogeneity during the drying process; the crystals cover a small range and do not affect the hydrophobicity. This effect should be avoided in practice. Figure 2c,d show SEM photographs of the coating at 100 nm and 50 nm, demonstrating the flatness of the coating at the microscopic level, so that the coating exhibits high transparency and smooth surface properties, whereby there will be no problem of a significant decrease in hydrophobicity due to the wear of the surface mechanics during routine cleaning and maintenance. The TEM images in Figure 3a,b reveal the microscopic morphology of the scraped coating after treatment under a transmission electron microscope. Selected area electron diffraction (SAED) of Figure 3c illustrates that the coating has an amorphous structure. Analysis of microscopic images of cross-sections containing coated glass yielded coating thicknesses in the range of 25–50 microns (Figure 4).

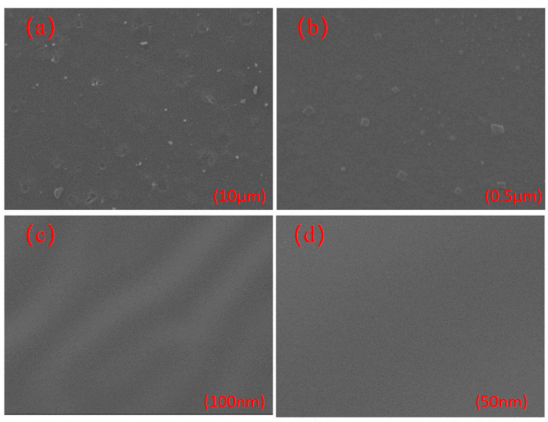

Figure 2. (**a**) SEM image of the coating at 10 μm. (**b**) SEM image of the coating at 0.5 μm. (**c**) SEM image of the coating at 100 nm. (**d**) SEM image of the coating at 50 nm.

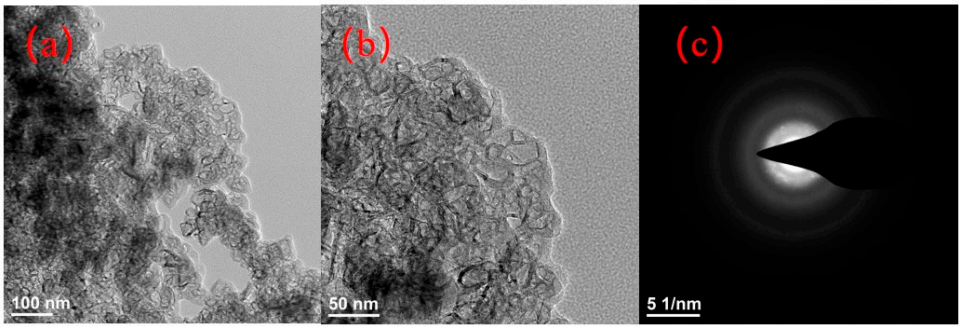

Figure 3. (**a**) TEM image of the coating at 100 nm. (**b**) TEM image of the coating at 50 nm. (**c**) Selected area electron diffraction (SAED) of the coating at 5/1 nm.

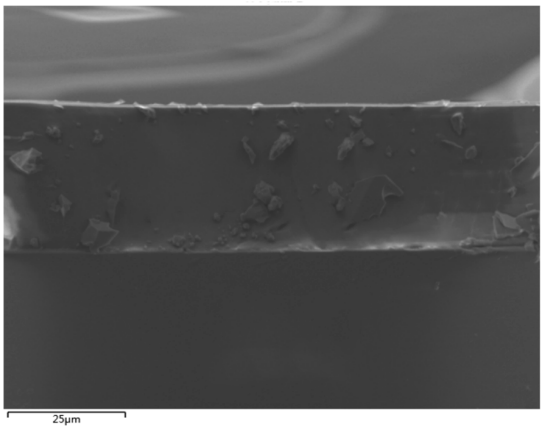

Figure 4. Scanning electron microscope image (25 microns) of a cross-section of coated glass, with the center strip being the coated portion and the lower portion of the out-of-focus region being the glass.

Figure 5 shows the FT-IR spectrum of the coated glass sheet. The strong and broad absorption band at 1053 cm^{-1} is assigned to the Si-O-Si anti-symmetric stretching vibration peak, while the peak at 784 cm^{-1} is attributed to the Si-O bond symmetric stretching vibration peak, and the peak at 1009 cm^{-1} belongs to the Si-OH bending vibration absorption peak. The strong and broad absorption band at 1053 cm^{-1}, the peak at 784 cm^{-1}, and the strong and broad peak at 3005 cm^{-1} indicate the presence of the silane coupling products prepared in the first step.

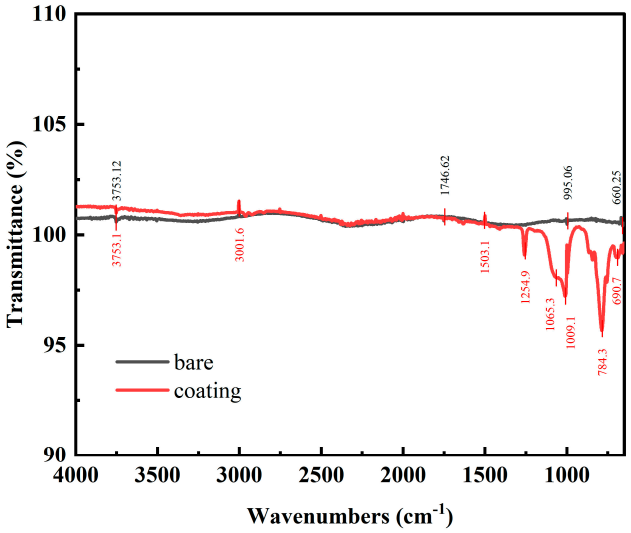

Figure 5. FT-IR spectra of bare glass and coated glass.

The weight percentages of each element in the overall coating were determined, as shown in Figure 6. The weight percentages of O, Si, and C were measured as 45.62%, 16.39%, and 36.69%, respectively.

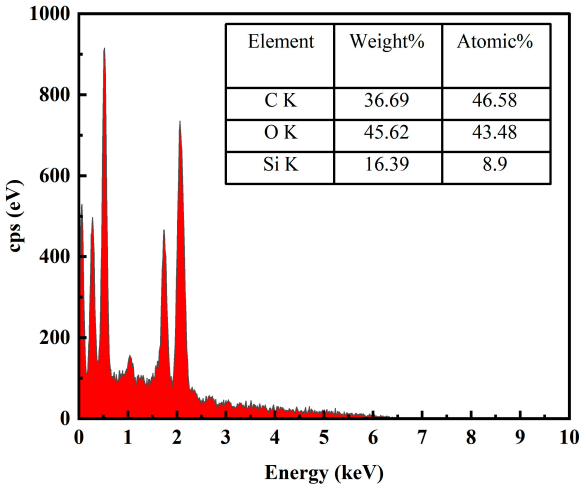

Figure 6. Energy dispersive spectroscopy (EDS) for coating. This test measures the percentage of C, O, and Si in the coating.

3.2. Wettability and Transparency Measurements

UV–vis spectrophotometer (UV–vis) measured the effect of coatings on light transmission and absorption of light. The contact angle meter (data physics OCA25, Nuremberg, Germany) quantitatively and visually measured the hydrophobic effect of the coating. The surface wettability of the films was characterized by the contact angle (WCA).

The static contact angle of the superhydrophobic thin film was measured by a data physics ORA 25 contact angle measurement system with a 10 μL water droplet, which varied from 0° to 180°. Five points were taken at different locations on the same piece of coated glass and the contact angle data were measured and averaged to obtain a contact angle at 122.78 degrees. The contact angles of different batches of coated glass were also measured: five coated pieces prepared from different batches were taken and the contact angles were found to be between 115° and 123°. The static contact angle for water on the prepared nanocoating was 122.78° (Figure 7), which suggests that the complex nanocoating is hydrophobic. The hydrophobicity property was also tested for other liquids, such as NaOH, H_2SO_4, HCL, acid violet 43, methyl blue, silicone oil, and edible oil, and the results showed that the complex nanocoating was hydrophobic for most of these liquids (Figure 7). It is worth noting that the static contact angle of bare glass is 38.73° (Figure 7), with a significant change in hydrophobicity compared to the coated glass.

The transparency and the durability responsible for the self-cleaning feature are two contradictory parameters; increasing one parameter strongly implies a decrease in the other [21]. For most coatings, a thicker layer means better durability, but a thicker layer causes a dramatic decrease in coating transparency, which is fatal for PV panel surface coatings, which require high transparency, so it is vital to choose the right thickness and enhance the transparency of the coating. We tested the transmission and absorption spectra of bare and coated glass plates in the wavelength range of 300–1000 nm (Figure 8). We selected three different sites on the same glass and scanned them in the range of 300–1000 nm, and averaged the transmission and absorption data over the entire range of scanned wavelengths. It can be calculated that the average transmittance of the coated glass panel was 0.69% higher than that of the bare glass panel, and the average absorption of light of the coated glass panel was 1.4% lower than that of the bare glass panel. These test data demonstrate that the coating does not affect light capture by the photovoltaic cells through the coated glass but also enhances the light absorption through the anti-reflection effect of the thin coating.

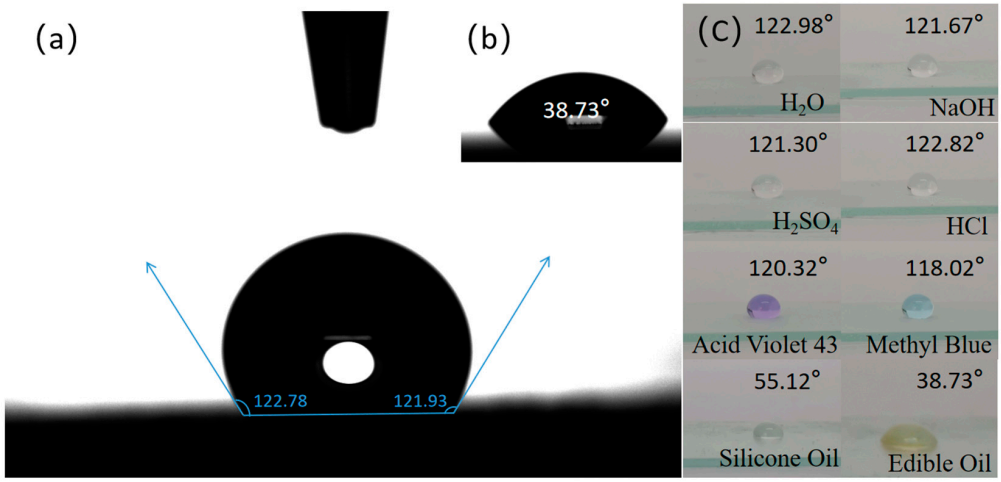

Figure 7. (**a**) The static contact angle for water on the prepared coating was 122.78 degrees. (**b**) The static contact angle for water on the bare glass. (**c**) Pictures of NaOH, H_2SO_4, HCl, acid violet 43, methyl blue, silicone oil, and edible oil on the prepared coating, separately.

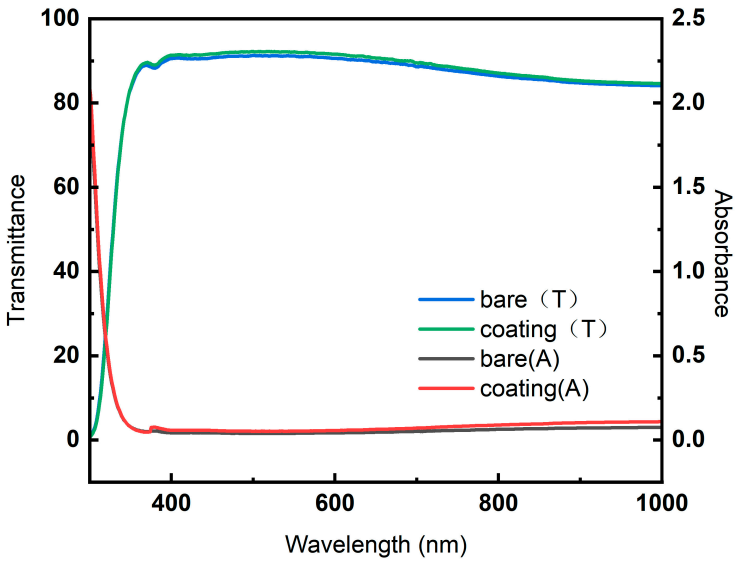

Figure 8. Transmission and absorption spectra of bare and coated glass plates in the wavelength range 300–1000 nm.

3.3. Mechanical Robustness and Self-Cleaning Performance of the Coating

In order to test the durability of the coatings, sandpaper friction tests were performed using sandpaper. To measure the self-cleaning ability of the coating, we collected dust from the local solar panels, spread it evenly on the surface of the coated glass sheets at an angle of 30°, and then water drops were sequentially placed on the surface to observe whether the pollutants could be removed by the water drops.

Reciprocating friction against sandpaper was adopted to evaluate the mechanical stability of the coatings [22]. The coated glass sheet (25.4 mm × 76.2 mm) was placed face down on the sandpaper (3M, 401Q, P2000, Shanghai, China), to which the pressure of a 1 kg weight was added, and then moved horizontally along the sandpaper; moving 10 cm on the sandpaper was counted as one cycle. As shown in Figure 9a, the static contact angle of the coating was tested after 10, 20, 50, 100, 150, and 200 friction cycles. The static contact angles of the six measurement points are around 122° (Figure 9b), which indicates that friction under this condition has a negligible effect on the hydrophobic properties of the coating. As shown in Figure 9c, the friction of the sandpaper on the coating caused

some rough structures on the coating surface, which may also be the reason for some small upward fluctuations in the contact angle.

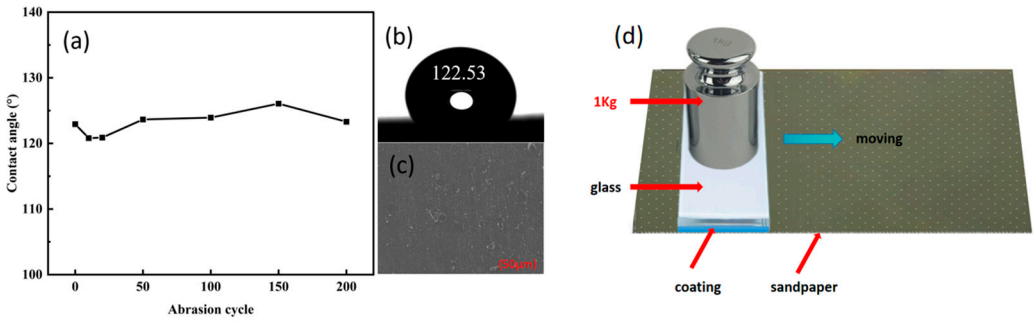

Figure 9. (**a**) Changes in hydrophobicity in the abrasion test against sandpaper. (**b**) Photographs of the coatings after 200 cycles (10 cm per cycle) under a 1 kg weight. (**c**) SEM photographs of the coatings after 200 cycles (10 cm per cycle) under a 1 kg weight. (**d**) Schematic diagram of sandpaper friction cycle experiment.

Most of the gradual deterioration in the hydrophobicity is due to the destruction of some protrusions on the coating surface, and the wear marks become more and more visible with increasing wear cycles [23,24]. In contrast, the nanoscale flat surface coating improved the hydrophobic degradation due to the destruction of the surface rough structure compared to most reported stable hydrophobic coatings, showing better mechanical stability and maintaining its hydrophobicity even after 200 cycles. Most of the gradual deterioration in hydrophobicity was due to the destruction of some protrusions on the coating surface and the wear marks became more and more visible with increasing wear cycles [25,26].

Self-cleaning performance can be verified by testing in practical situations [27]. The coated substrate was placed at an angle of approximately 30° relative to the horizontal plane. The dust collected on the local solar panel was spread evenly on the coated glass sheet, and then an aqueous solution of acidic violet 43 was applied to the glass drop by drop until all the dust was washed off the glass (Figure 10). Figure 10d shows uncoated glass with dust evenly spread on it. Multiple drops of water solution were applied. It can be seen that the dust is still not cleaned on the two water trails. The aqueous solution containing surfactants was found to be better for cleaning the dust, making the cleaning process faster and more water-efficient, probably due to the oily organic component of the local dust.

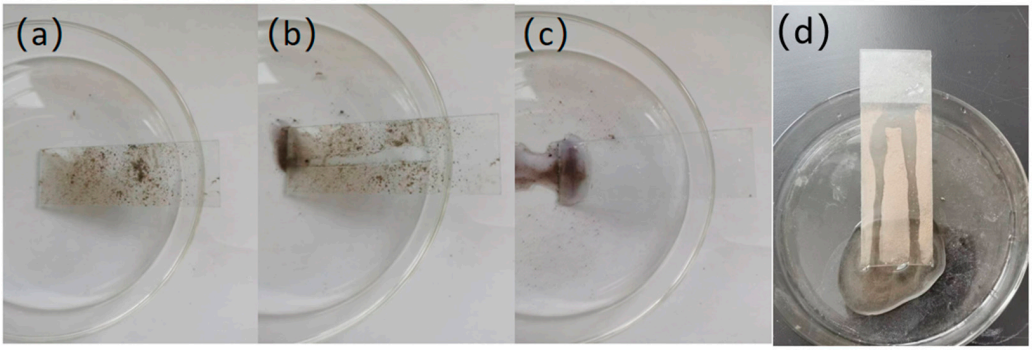

Figure 10. Self-cleaning performance of coated glass. (**a**) The glass sheet is sprinkled lightly with dust collected from local solar panels. (**b**) A dropper is used to put three drops of water on the plate. (**c**) A small amount of water is used to clean off the dust. (**d**) Comparison with uncoated glass panel: the cleaning effect of surface dust with three drops of water.

Studies have shown that droplets have the best bouncing performance on random rough surfaces [28]. However, the coatings we prepared tended to be smooth surfaces, so the droplet bouncing was not obvious, and the droplet trajectory tended to be close to a straight line when cleaning, which is relatively more water-efficient.

3.4. Test of the Coating on Real Photovoltaic Panel

The coating was applied to a photovoltaic panel and the panel was placed in an outdoor environment for 3 weeks to measure the amount of dust accumulation and the effect on the efficiency of the photovoltaic panel in generating electricity.

The photovoltaic panels were SYSP-type monocrystalline solar panels (18 V, 20 W) produced by Shenzhen Xiangri Solar Energy Technology Co. (Shenzhen, China), with specifications of 300 cm × 410 cm × 17 cm, and were tested by a Tes-1333 solar irradiator, PVT801 solar photovoltaic panel tester, electronic scales, and non-contact infrared temperature measuring gun. Two solar panels of the same specifications, covered with coated and uncoated glass, were placed in the outdoor environment in Beijing. The solar radiation, solar panel ash accumulation, current, voltage, power, temperature, and other parameters were tested every day at 12:00 noon for three weeks, from 25 June 2023 to 16 July 2023. The PV panels were not rained on during the experiment. The density of dust deposition on the photovoltaic module decreases with the increase in tilt angle when it faces the wind [29]. Considering the convenience of measurement and the optimal tilt angle of the site, the tilt angle of the PV panel was set to 60°.

With the passage of time, an increase in the density of dust accumulated on the surfaces was observed and the efficiency of the solar panels was calculated to decrease gradually. Due to the difference in the dust density on each panel, the average dust densities of the bare and coated glass increased to 22.76 g/m^2 and 14.63 g/m^2 from 0 g/m^2, respectively, this was due to the self-cleaning property of the coating, which reduced the amount of dust accumulated on the glass surface.

In Figure 11a, an image of the ash accumulation on the fifth day is shown, the image on the left-hand side is the coated PV panel and the one on the right-hand side is the uncoated PV panel, and by comparing them it can be seen that the amount of ash accumulation on the left-hand side is higher than that on the right-hand side. Figure 11b is an image of the ash accumulation on the tenth day. On the tenth day some light rain fell. Comparing the two solar panels, it can be clearly seen that the right-hand side of the PV panel is cleaner than the uncoated PV panel, and the left-hand side of the PV panel has patches of stains on the PV panel. The above comparison shows that the coated PV panels have significant self-cleaning properties.

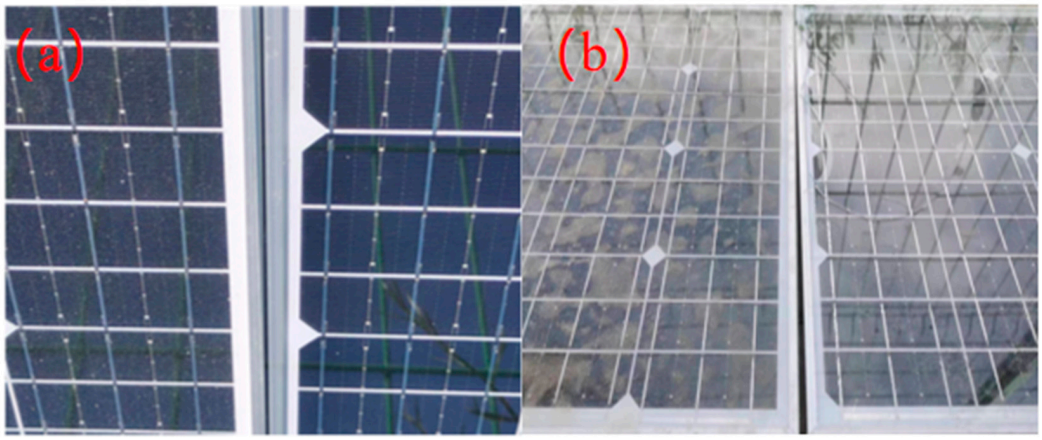

Figure 11. (**a**) Dust accumulation image at day 5, with the left PV panel being the uncoated control group and the right PV panel being the coated experimental group. (**b**) Image of ash accumulation after rain at day 10, with the left PV panel being the uncoated control group and the right PV panel being the coated experimental group.

It can also be concluded from Figure 12 that the density of dust accumulated by the coated and bare solar panels is also different, with the dust density curve of the uncoated solar panels having a smaller slope and the dust density curve of the coated solar panels having a more significant slope, indicating that the coating has the ability to mitigate the accumulation of dust on the photovoltaic panels.

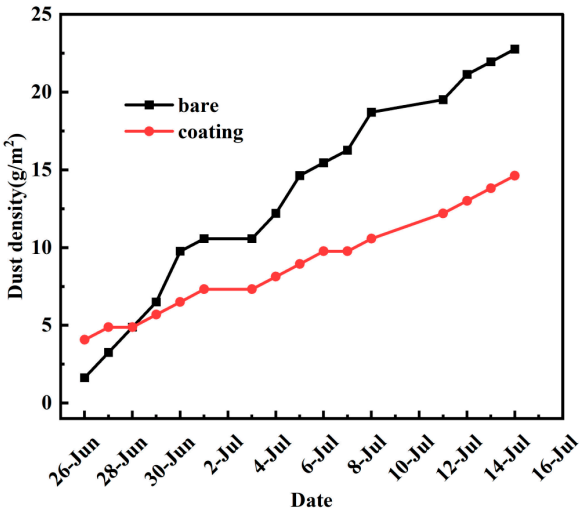

Figure 12. Dust density (g/m^2) accumulated by bare and coated solar panels over 3-week period.

As shown in Figures 13 and 14 the I–V and P–V fitting curves are plotted from the current, voltage, and power data obtained from the three-week test. The maximum power of the bare panel is 13.79 (W), and the maximum power of the coated panel is 13.99 (W); the minimum power of the bare panel is 4.91 (W), and that of the coated panel is 5.56 (W). It can be seen that the coating has a positive effect on the power of the PV panels.

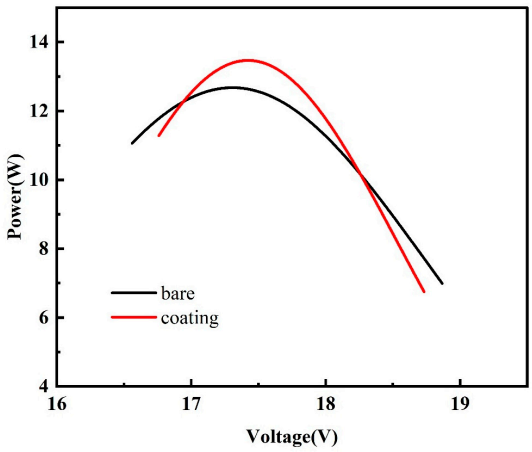

Figure 13. The P–V curve fitted to data from the bare and coated solar panels over 3-week period.

The electrical output power was calculated using Watt's law according to Equation (1).

$$Ppv = V \times I, \tag{1}$$

where V is the PV panel voltage (V), and I is the PV panel current (I.).

The efficiency of the PV panels (ηpv) was calculated as the ratio of the PV panel's output power and the input solar power (Equation (2)) [30].

$$\eta = \frac{V \times I}{A \times G} \tag{2}$$

where A is the PV panel surface area (m^2), and G is the intensity of solar radiation (W/m^2).

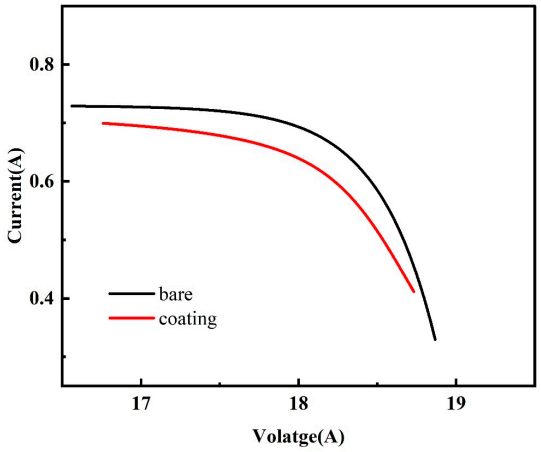

Figure 14. The I–V curve fitted to data from the bare and coated solar panels over 3-week period.

Through testing, we obtained the daily solar irradiance data, PV panel current, PV panel voltage, temperature, power, and other data, which were used in the calculation of Equations (1) and (2).

The daily 3-week panel efficiency data of the solar panels are shown in Figure 15. From the data, it can be seen that at the beginning the efficiency of the coated PV panels was about the same as that of the uncoated PV panels, but on the seventh day, the efficiency of the coated PV panels was higher than that of the uncoated PV panels. At the end of three weeks, the efficiency of the coated PV panels was higher than the uncoated PV panels by 1.11%. In three weeks, the efficiency of the uncoated PV panels decreased by 3.8%, while the efficiency of the coated PV panels decreased by only 1.48%. It can be seen in the figure that the rate of decrease in the efficiency of the uncoated PV panels was significantly larger than that of the coated PV panels. The above comparison shows that the coated PV panels have obvious self-cleaning performance.

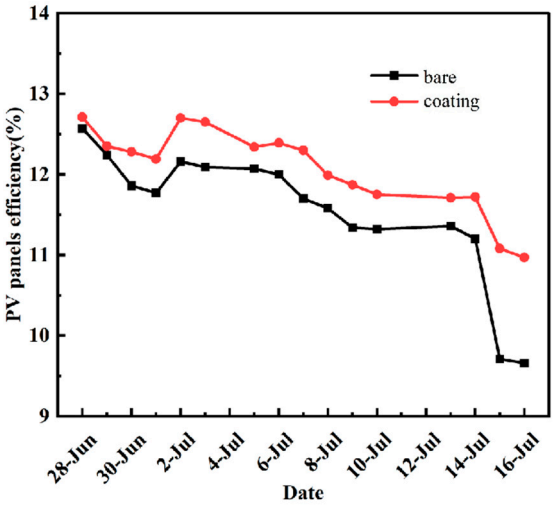

Figure 15. Panel efficiency (%) tested on bare and coated solar panels over 3-week period.

By comparing the temperature data of the 6th, 16th, and 22nd days with the same solar irradiation intensity of 880 W/m^2–890 W/m^2, it is found that there is a significant increase in the temperature, which indicates that the accumulation of ash has a negative impact on the surface temperature of the PV panel, and the self-cleaning property of the coating has a positive impact on the PV panel itself, which is important for improving the lifetime of the PV panel and reducing the possibility of hot spots formed due to high temperatures.

4. Discussion

From the perspective of bionics, researchers have found that the hydrophobic phenomenon on the surface of the lotus leaf has the effect of self-cleaning [31]: due to the high contact angle (>150°), water drops readily roll off the lotus leaf surface, collecting dirt particles. More and more researchers are studying the principle of hydrophobicity and have found that the strength of hydrophobicity is mainly dependent on the surface roughness structure and compound hydrophobic groups [32]. Nowadays, many superhydrophobic surfaces have been researched, and the contact angle can be as high as 170 degrees [33], but most of them mainly rely on the rough structure to achieve the purpose of hydrophobicity [34], and the construction of rough surfaces needs to go through various chemical and physical treatments [35,36], which leads to the complexity of the coating process, and the high cost. When we want to apply the coating on an actual PV panel's surface, the durability, transparency, preparation cost, and the coating process become critical issues. The rough structure will be smoothed out with mechanical friction and lose its hydrophobic effect, which leads to poor durability. Compounds containing more hydrophobic groups are white or opaque, and an inhomogeneous rough structure also leads to lower transparency.

This paper proposed constructing a hydrophobic coating with a smooth surface structure, and we designed and synthesized a resin composite film containing modified silica components, mainly by using an organic/inorganic composite material approach. Hydrophobicity is achieved by relying only on the hydrophobic groups of the compounds.

A smooth surface prevents scratches. The direct damage to the paint film caused by scratches is obvious. When a sharp object rubs across the film, causing irreversible deformation or even a direct cut through, this is a scratch to the film. The addition of a smoothing additive improves the smoothness of the surface and significantly reduces this damage. The principle is to make objects slide across the surface instead of scratching the paint film. Smooth surfaces demonstrate significant scratch resistance.

If the interaction force between the chain segments of the smoothing additives are weak, then the scratch resistance is significantly improved. Organically modified polysiloxanes containing a high proportion of polydimethylsiloxane chain segments exhibit particularly weak interaction forces, both with each other and with other materials, which makes them ideal smoothing additives. Organically modified silicones minimize the unevenness of the film surface and help coatings to form a very smooth surface. During the drying process, the organomodified siloxanes continue to accumulate on the surface of the coating film and a very slippery film is formed. Fluid lubrication occurs at this point and slipperiness can be significantly improved.

Firstly, the microscopic morphology was tested and the surface of the coating was found to be smooth at the micrometer level. After testing the chemical composition, the validation and testing program was designed based on the actual requirements for self-cleaning coatings on PV panel surfaces.

The coatings on PV panels can be evaluated by (1) hydrophobicity; (2) transparency; (3) durability; and (4) economy.

Hydrophobicity is part of the self-cleaning ability, so we designed the experiment to measure the contact angle to prove the hydrophobicity; the water contact angle could reach 122°.

Transparency is a key indicator for the efficiency of PV panels, if the transparency is low it will greatly affect the efficiency of PV panels. So we designed an experiment using ultraviolet and visible spectrophotometry to test the light transmittance, and found that it was 0.69% higher than pure glass.

Durability is a more prominent issue for coatings in practical use. If the durability is not good, the hydrophobicity will be gradually lost with daily mechanical wear and tear. After the coating loses its effectiveness, maintenance and re-coating at a later stage are costly and labor intensive. Therefore, we designed a sandpaper friction experiment to prove that the coating had the ability to resist abrasion under daily mechanical abrasion.

Economically, we accounted for the cost of the coating. One square meter of glass panel requires 0.1 L of coating. The cost of one square meter of glass panel coating based on industrial-grade raw materials was RMB 2.5–3.5. The total cost, including labor and coating process costs, was initially estimated to be less than RMB 10, which is low compared to most paints on the market.

Although this study revealed important discoveries, there are also limitations. Firstly, the contact angle of the smooth surface is not as high as the contact angle achieved using the traditional method of constructing rough surfaces, and there is still room for improvement in terms of the hydrophobic effect. Secondly, the hydrophobic surfaces are theoretically anti-icing [37], but this effect has not been tested considering that most PV devices are installed in arid and dusty areas. Third, in outdoor practical application weather resistance is also an important evaluation index [38], but in arid and dusty areas corrosive substances have less impact, and the impact period is too long, so this could not be tested. Finally, in terms of practical application testing, due to the conditions there were few samples and a short cycle. It is believed that with more samples and a longer cycle the advantages of the coating will be more obvious.

One important future direction of self-cleaning coatings is the more comprehensive improvement of overall performance in terms of durability and weathering, as well as a summary of the principles. The experimental research results will hopefully serve as useful feedback information for improvements in self-cleaning coating work.

5. Conclusions

In this study, a preparation method of hydrophobic self-cleaning film for polycrystalline PV modules with good weatherability is proposed. According to a series of investigations, the following conclusions are drawn.

By preparing fluorine-containing permeation-enhancing resin films, the surface morphology shows that the films have micrometer-level flat surfaces, which improves the problem of reduced hydrophobicity due to the wear and tear of the hydrophobic rough structure on the surface of conventional hydrophobic coatings with daily use. The static contact angle of the film is 122.78 degrees; it can be calculated that the average transmittance of the coated glass panel is 0.69% higher than that of the bare glass panel, and mechanical wear and tear has less impact on the hydrophobicity. Experiments under the actual working conditions of PV panels also show that the coating is indeed self-cleaning, which can improve the efficiency of the PV panels and lower the temperature of the PV panels, thus reducing the expenditure on cleaning and maintenance and improving the service life of the PV panels. This technique provides a new opportunity in the practical application of self-cleaning film on photovoltaic glass covers.

Author Contributions: Conceptualization, Y.W., H.L. and S.W.; methodology, R.G.; validation, S.W., Y.W. and H.L.; formal analysis, R.G.; investigation, R.G., B.W. and Q.Z.; data curation, R.G.; writing—original draft preparation, R.G.; writing—review and editing, S.W., Y.W., B.W. and Q.Z.; supervision, S.W., Y.W. and H.L.; funding acquisition, S.W., Y.W. and H.L. All authors have read and agreed to the published version of the manuscript.

Funding: The authors appreciate the financial supports provided by National Key Research and Development Program of China (No. 2023YFB4102704), the financial support provided by the National Oversea High-level Talents Program of China, National Natural Science Foundation of China (No. 52266017) and the Major Project of the National Social Science Foundation of China (No. 21&ZD133). It is also supported by the Xinjiang Natural Science Fund for Distinguished Young Scholars (No. 2021D01E08), the Xinjiang Regional Coordination Special Project-International Science and Technology Cooperation Program (No. 2022E01026), the Xinjiang Major Science and Technology Special Project (No. 2022A01002-2, 2022A01007-1, 2023A01005-02), the Xinjiang Key Research and development Project (No. 2022B03028-2, No. 2022B01033-2, No. 2022B01022-1, No. 2022B01020-4), the Central Guidance on Local Science and Technology Development Project (No. ZYYD2022C16), the Innovation Team Project of Xinjiang University (500122006021) and High-

level Talents Project of Xinjiang University (No. 100521001), Central Government Funds for Local Scientific and Technological Development (Grant No. XZ202101YD0019C).

Institutional Review Board Statement: Not applicable.

Informed Consent Statement: Not applicable.

Data Availability Statement: The data presented in this study are available on request from the corresponding author.

Conflicts of Interest: The authors declare no conflicts of interest.

References

1. Laxmikant, D.J.; Ganesan, S.; Umesh, A.; Keval, N.; Kiran, S.; Manzoore Elahi, M.S.; Fayaz, H.; El-Shafay, A.S.; Kalam, M.A.; Salwa, B.; et al. Comprehensive review of environmental factors influencing the performance of photovoltaic panels: Concern over emissions at various phases throughout the lifecycle. *Environ. Pollut.* **2023**, *326*, 121474. [CrossRef]
2. Huang, Z.S.; Shen, C.; Fan, L.; Ye, X.; Shi, X.; Li, H.; Zhang, Y.; Lai, Y.; Quan, Y.Y. Experimental investigation of the anti-soiling performances of different wettability of transparent coatings: Superhydrophilic, hydrophilic, hydrophobic and superhydrophobic coatings. *Sol. Energy Mater. Sol. Cells* **2021**, *225*, 111053. [CrossRef]
3. Sanaz, G.; Kenneth, I. The effect of weather conditions on the efficiency of PV panels in the southeast of UK. *Renew. Energy* **2014**, *69*, 50–59. [CrossRef]
4. He, B.; Lu, H.; Zheng, C.; Wang, Y. Characteristics and cleaning methods of dust deposition on solar photovoltaic modules-A review. *Energy* **2023**, *263*, 126083. [CrossRef]
5. Jaszczur, M.; Koshti, A.; Nawrot, W.; Sędor, P. An investigation of the dust accumulation on photovoltaic panels. *Environ. Sci. Pollut. Res.* **2020**, *27*, 2001–2014. [CrossRef] [PubMed]
6. Rudnicka, M.; Klugmann-Radziemska, E. Soiling Effect Mitigation Obtained by Applying Transparent Thin-Films on Solar Panels: Comparison of Different Types of Coatings. *Materials* **2021**, *14*, 964. [CrossRef] [PubMed]
7. Deepanjana, A.; Raghunath, B.; Harish, C.B. A state-of-the-art review on the multifunctional self-cleaning nanostructured coatings for PV panels, CSP mirrors and related solar devices. *Renew. Sustain. Energy Rev.* **2022**, *159*, 112145. [CrossRef]
8. Lu, H.; Zheng, C. Comparison of Dust Deposition Reduction Performance by Super-Hydrophobic and Super-Hydrophilic Coatings for Solar PV Cells. *Coatings* **2022**, *12*, 502. [CrossRef]
9. Yuan, Y.; Lee, T.R. Contact Angle and Wetting Properties. In *Surface Science Techniques*; Bracco, G., Holst, B., Eds.; Springer: Berlin/Heidelberg, Germany, 2013; pp. 3–34.
10. Yusuf, N.C.; Aritra, G.; Senthilarasu, S.; Tapas, K.M. Dust and PV Performance in Nigeria: A review. *Renew. Sustain. Energy Rev.* **2020**, *121*, 109704. [CrossRef]
11. Cecilia, A.-S.; Maider, M.; Jiri, N.; Naiara, Y.; Asier, S.; Marta, B.; Oihana, Z.; Agnieszka, T. Mechanical properties and field performance of hydrophobic antireflective sol-gel coatings on the cover glass of photovoltaic modules. *Sol. Energy Mater. Sol. Cells* **2020**, *216*, 110694. [CrossRef]
12. Zhang, J.; Ai, L.; Lin, S.; Lan, P.; Lu, Y.; Dai, N.; Tan, R.; Fan, B.; Song, W. Preparation of humidity, abrasion, and dust resistant antireflection coatings for photovoltaic modules via dual precursor modification and hybridization of hollow silica nanospheres. *Sol. Energy Mater. Sol. Cells* **2019**, *192*, 188–196. [CrossRef]
13. Wang, D.; Sun, Q.; Hokkanen, M.J.; Zhang, C.; Lin, F.-Y.; Liu, Q.; Zhu, S.-P.; Zhou, T.; Chang, Q.; He, B.; et al. Design of robust superhydrophobic surfaces. *Nature* **2020**, *582*, 55–59. [CrossRef]
14. Aritra, G. Potential of building integrated and attached/applied photovoltaic (BIPV/BAPV) for adaptive less energy-hungry building's skin: A comprehensive review. *J. Clean. Prod.* **2020**, *276*, 123343. [CrossRef]
15. Tian, W.; Li, C.; Liu, K.; Ma, F.; Chu, K.; Tang, X.; Wang, Z.; Yue, S.; Qu, S. Fabrication of Transferable and Micro/Nanostructured Superhydrophobic Surfaces Using Demolding and iCVD Processes. *ACS Appl. Mater. Interfaces* **2023**, *15*, 2368–2375. [CrossRef]
16. Liu, S.; Liu, X.; Latthe, S.S.; Gao, L.; An, S.; Yoon, S.S.; Liu, B.; Xing, R. Self-cleaning transparent superhydrophobic coatings through simple sol–gel processing of fluoroalkylsilane. *Appl. Surf. Sci.* **2015**, *351*, 897–903. [CrossRef]
17. Pawar, P.G.; Xing, R.; Kambale, R.C.; Kumar, A.M.; Liu, S.; Latthe, S.S. Polystyrene assisted superhydrophobic silica coatings with surface protection and self-cleaning approach. *Prog. Org. Coat.* **2017**, *105*, 235–244. [CrossRef]
18. Umer, M.; Fahad, A.A.-S.; Yilbas, B.S.; Salhi, B.; Ahmed, S.H.A.; Mohammad, K.H. Superhydrophobic surfaces with antireflection properties for solar applications: A critical review. *Sol. Energy Mater. Sol. Cells* **2016**, *157*, 604–623. [CrossRef]
19. Zhi, J.; Zhang, L.-Z. Durable superhydrophobic surfaces made by intensely connecting a bipolar top layer to the substrate with a middle connecting layer. *Sci. Rep.* **2017**, *7*, 9946. [CrossRef] [PubMed]
20. Dalawai, S.P.; Aly, M.A.S.; Latthe, S.S.; Xing, R.; Sutar, R.S.; Nagappan, S.; Ha, C.-S.; Sadasivuni, K.K.; Liu, S. Recent Advances in durability of superhydrophobic self-cleaning technology: A critical review. *Prog. Org. Coat.* **2020**, *138*, 105381. [CrossRef]
21. Wang, P.; Wang, H.; Li, J.; Ni, L.; Wang, L.; Xie, J. A superhydrophobic film of photovoltaic modules and self-cleaning performance. *Sol. Energy* **2021**, *226*, 92–99. [CrossRef]
22. Yao, L.; Sanjayan, S.; Jinlong, S.; Colin, R.C.; Claire, J.C.; Ivan, P.P. Robust self-cleaning surfaces that function when exposed to either air or oil. *Science* **2015**, *347*, 1132–1135. [CrossRef]

23. Tayel, S.A.; Abu El-Maaty, A.E.; Mostafa, E.M.; Elsaadawi, Y.F. Enhance the performance of photovoltaic solar panels by a self-cleaning and hydrophobic nanocoating. *Sci. Rep.* **2022**, *12*, 21236. [CrossRef]
24. Ghanbari, T. Hot spot detection and prevention using a simple method in photovoltaic panels. *IET Gener. Transm. Distrib.* **2017**, *11*, 883–890. [CrossRef]
25. Liu, M.; Hou, Y.; Li, J.; Tie, L.; Guo, Z. An all-water-based system for robust superhydrophobic surfaces. *J. Colloid Interface Sci.* **2018**, *519*, 130–136. [CrossRef]
26. Liu, M.; Hou, Y.; Li, J.; Tie, L.; Peng, Y.; Guo, Z. Inorganic adhesives for robust, self-healing, superhydrophobic surfaces. *J. Mater. Chem. A* **2017**, *5*, 19297–19305. [CrossRef]
27. Liu, S.; Liu, S.; Wang, Q.; Zuo, Z.; Liang, X. Design and synthesis of robust superhydrophobic coating based on epoxy resin and polydimethylsiloxane interpenetrated polymer network. *Prog. Org. Coat.* **2023**, *175*, 107336. [CrossRef]
28. Lu, S.; Lu, H.; Hu, L.; Wang, X. A numerical investigation of droplet bouncing behaviors on the superhydrophobic surfaces with different micro-structures. *Case Stud. Therm. Eng.* **2023**, *43*, 102728. [CrossRef]
29. Lu, H.; He, B.; Zhao, W. Experimental study on the super-hydrophobic coating performance for solar photovoltaic modules at different wind directions. *Sol. Energy* **2023**, *249*, 725–733. [CrossRef]
30. Wang, J.; Li, K.; Zhang, J.; Feng, J. Transparent and superhydrophobic FHA/SiO2 coatings with obvious anti-soiling performance for photovoltaic modules. *Prog. Org. Coat.* **2023**, *183*, 107679. [CrossRef]
31. Jing, X.; Guo, Z. Biomimetic super durable and stable surfaces with superhydrophobicity. *J. Mater. Chem. A* **2018**, *6*, 16731–16768. [CrossRef]
32. Latthe, S.S.; Sutar, R.S.; Kodag, V.S.; Bhosale, A.K.; Kumar, A.M.; Kumar Sadasivuni, K.; Xing, R.; Liu, S. Self—Cleaning superhydrophobic coatings: Potential industrial applications. *Prog. Org. Coat.* **2019**, *128*, 52–58. [CrossRef]
33. Zhang, L.; Zhou, A.G.; Sun, B.R.; Chen, K.S.; Yu, H.-Z. Functional and versatile superhydrophobic coatings via stoichiometric silanization. *Nat. Commun.* **2021**, *12*, 982. [CrossRef]
34. Zhang, J.; Ai, L.; Xu, Y.; Lou, X.; Lan, P.; Lu, Y.; Dai, N.; Song, W. Preliminary studies of effects of surface morphology and chemistry of silica-based antireflection coatings on anti-soiling performance under Ningbo's climate. *Sol. Energy* **2020**, *205*, 302–309. [CrossRef]
35. Abbasi, S.; Ruankham, P.; Passatorntaschakorn, W.; Khampa, W.; Musikpan, W.; Bhoomanee, C.; Liu, H.; Wongratanaphisan, D. A new single-step technique to fabricate transparent hydrophobic surfaces utilizable in perovskite solar cells. *Appl. Surf. Sci.* **2022**, *613*, 155969. [CrossRef]
36. Rombaut, J.; Fernandez, M.; Mazumder, P.; Pruneri, V. Nanostructured Hybrid-Material Transparent Surface with Antireflection Properties and a Facile Fabrication Process. *ACS Omega* **2019**, *4*, 19840–19846. [CrossRef]
37. Motahareh Borzou, E.; Akbar, E.; Saeed Reza, B. Transparent hydrophobic, self-cleaning, anti-icing and anti-dust nano-structured silica based thin film on cover glass solar cell. *J. Non-Cryst. Solids* **2022**, *583*, 121479. [CrossRef]
38. Narendra, C.; Ganesh, K.; Easwaramoorthi, R.; Sudhanshu, M.; Anil, K.; Shanmugasundaram, S. Ambient condition curable, highly weather stable anti-soiling coating for photovoltaic application. *Sol. Energy Mater. Sol. Cells* **2021**, *230*, 111203. [CrossRef]